

# Biocompatibility and biosafety of butterfly wings for the clinical use of tissue-engineered nerve grafts

<https://doi.org/10.4103/1673-5374.303041>

Shu Wang<sup>1</sup>, Miao Gu<sup>2</sup>, Cheng-Cheng Luan<sup>1</sup>, Yu Wang<sup>1</sup>, Xiaosong Gu<sup>1</sup>, Jiang-Hong He<sup>1,\*</sup>

Date of submission: May 15, 2020

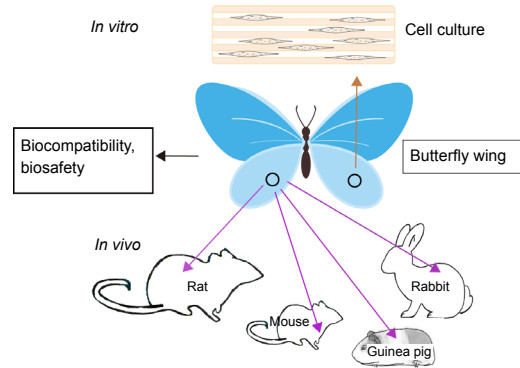
Date of decision: June 18, 2020

Date of acceptance: July 16, 2020

Date of web publication: January 7, 2021

## Graphical Abstract

Natural butterfly wings exhibited good *in vitro* biocompatibility with Schwann cells and dorsal root ganglion neurons and good *in vivo* histocompatibility and biosafety.



## Abstract

In a previous study, we used natural butterfly wings as a cell growth matrix for tissue engineering materials and found that the surface of different butterfly wings had different ultramicrostructures, which can affect the qualitative growth of cells and regulate cell growth, metabolism, and gene expression. However, the biocompatibility and biosafety of butterfly wings must be studied. In this study, we found that Sprague-Dawley rat dorsal root ganglion neurons could grow along the structural stripes of butterfly wings, and Schwann cells could normally attach to and proliferate on different species of butterfly wings. The biocompatibility and biosafety of butterfly wings were further examined through subcutaneous implantation in Sprague-Dawley rats, intraperitoneal injection in Institute of Cancer Research mice, intradermal injection in rabbits, and external application to guinea pigs. Our results showed that butterfly wings did not induce toxicity, and all examined animals exhibited normal behaviors and no symptoms, such as erythema or edema. These findings suggested that butterfly wings possess excellent biocompatibility and biosafety and can be used as a type of tissue engineering material. This study was approved by the Experimental Animal Ethics Committee of Jiangsu Province of China (approval No. 20190303-18) on March 3, 2019.

**Key Words:** biocompatibility; biomaterials; biosafety; butterfly wings; dorsal root ganglion; neurons; Schwann cells; tissue engineering

Chinese Library Classification No. R456; R741; R622+.3

## Introduction

Materials are key elements of tissue engineering and cell-based therapies (Guthrie et al., 2013; Facklam et al., 2020; Vermeulen and de Boer, 2020). Various materials, including bioinert and bioactive materials, have been applied clinically to repair diverse tissues and organs (Yi et al., 2019). Synthetic non-degradable materials, such as silicone and polyethylene glycol, and synthetic degradable materials, such as polyglycolic acid, polylactic acid, and poly (lactin-co-glycolic acid), have been widely applied in the fields of tissue engineering and regenerative medicine (Yu et al., 2017; Qian et al., 2019). Recently, naturally derived materials have begun to attract attention (Ghosh et al., 2019). Naturally derived materials present many advantages, such as abundant resources, excellent biological performance, and similar mechanical properties to tissues and organs, and thus have been

developed for many clinical applications.

Chitosan, a natural, polycationic, linear polysaccharide that is derived from chitin, has commonly been used in the construction of neural scaffolds and the treatment of peripheral nerve injury (Wang et al., 2005; Stenberg et al., 2016; Bhatt et al., 2017; Crosio et al., 2019; Dietzmeier et al., 2020; Yu et al., 2020). Butterfly wings are natural biomaterials composed of chitin (Elbaz et al., 2017), which possess fine micro-/nano-surface structures and have been utilized as a biomimetic material (Mu et al., 2013; Zhang et al., 2015). In our previous study, butterfly wings were collected from *Morpho menelaus* (*M.m.*) and *Papilio ulysses telegonus* (*P.u.t.*), two types of butterflies with divergent wing-surface topographies, to observe the influence of wing structures and surface features on Schwann cell arrangements. Our results indicated that Schwann cells cultured on *M.m.* wings,

<sup>1</sup>Key Laboratory for Neuroregeneration of Jiangsu Province and Ministry of Education, Co-innovation Center of Neuroregeneration, Nantong University, Nantong, Jiangsu Province, China; <sup>2</sup>Department of Basic Medicine, Chengde Medical College, Chengde, Hebei Province, China

\*Correspondence to: Jiang-Hong He, PhD, hejh@ntu.edu.cn.

<https://orcid.org/0000-0002-5185-7982> (Jiang-Hong He)

**Funding:** This work was supported by the National Natural Science Foundation of China, No. 31971276, and the Natural Science Foundation of Jiangsu Higher Education Institutions of China (Major Program), No. 19KJA320005 (both to JHH).

**How to cite this article:** Wang S, Gu M, Luan CC, Wang Y, Gu X, He JH (2021) Biocompatibility and biosafety of butterfly wings for the clinical use of tissue-engineered nerve grafts. *Neural Regen Res* 16(8):1606-1612.

the surfaces of which are composed of grooves, exhibited a regular sorting pattern, whereas Schwann cells cultured on *P.u.t.* wings, the surfaces of which are composed of micro-/nano-concaves, exhibited randomized growth (He et al., 2018). These outcomes suggested that *M.m.* wings may be suitable for Schwann cell growth and peripheral nerve repair (He et al., 2018).

For the successful regeneration and functional recovery of injured peripheral nerves, implanted biomaterials should have good biocompatibility not only with Schwann cells but also with neuronal axons. Therefore, in the current study, dorsal root ganglion (DRG) neurons were collected and cultured on *M.m.* wings to determine the biocompatibility of *M.m.* wings with DRG neurons. The proliferation and attachment of Schwann cells on butterfly wings were also evaluated. Moreover, butterfly wings or butterfly wing extracts were applied to various types of animals, including Sprague-Dawley rats, Institute of Cancer Research (ICR) mice, rabbits, and guinea pigs, to examine the biosafety of these materials. The biocompatibility and biosafety evaluation of butterfly wings would increase the clinical applications of natural materials that present with biomimetic structures.

## Materials and Methods

### Animals

Embryonic day 14 (E14), specific-pathogen-free, Sprague-Dawley rats were used to obtain DRG cultures. Postnatal, 1–2-day-old, specific-pathogen-free, wild-type, Sprague-Dawley rats ( $n = 20$ ) and green fluorescent protein-transgenic Sprague-Dawley rats ( $n = 20$ ) were used to obtain Schwann cell cultures. A total of 36 adult male Sprague-Dawley rats (specific-pathogen-free level weighing 200–250 g), 28 adult ICR mice (specific-pathogen-free level, half female and half male, weighing 18–20 g), nine adult white rabbits (6-month-old, clean level, weighing 2.5–3 kg), and 32 healthy adult guinea pigs (clean level, 1.5-year-old, weighing 350–400 g) were obtained from the Experimental Animal Center of Nantong University, China (license Nos. SYXK [Su] 2017-0045 and SYXK [Su] 2017-0046).

All procedures were conducted in accordance with the Institutional Animal Care guidelines of Nantong University and were approved by the Experimental Animal Ethics Committee of Jiangsu Province, China (approval No. 20190303-18) on March 3, 2019.

### Butterfly wing fabrication

*M.m.* and *P.u.t.* wings, purchased from Beijing Yuxiao Media (Beijing, China), were prepared as described previously (He et al., 2018). Briefly, butterfly wings were exposed to 1 M HCl for 2 hours and 2 M NaOH overnight to increase their hydrophilic properties. Treated butterfly wings were then sterilized by overnight immersion in 70% ethanol and ultraviolet radiation (15 minutes).

Sterilized butterfly wings were soaked in Dulbecco's modified Eagle's medium (Invitrogen, Carlsbad, CA, USA) for 72 hours at 37°C to collect different concentrations of butterfly wing extracts (3, 6, and 12 cm<sup>2</sup>/mL).

### Chitosan film fabrication

Chitosan, a widely used biomaterial in tissue engineering with no detectable side effects, was used as a control. Chitosan (Nantong Water Products Institute, Nantong, China) with a deacetylation degree of 92.5% and a viscosity of 0.11 Pa·s was dissolved in 2% acetic acid, added to a culture dish, and frozen into a film. Frozen chitosan films were neutralized with 5% NaOH for 30 minutes, washed with distilled water, soaked overnight in Dulbecco's modified Eagle's medium containing 1% penicillin and streptomycin (Invitrogen), and coated with

poly-L-lysine hydrobromide for subsequent studies.

### DRG culture

DRGs were dissected from embryonic day (E) 14 rats, as previously described (Liu et al., 2019). Isolated DRGs were digested with 0.5 mg/mL collagenase (Roche, Basel, Switzerland) for 2 hours and 0.125% trypsin (Thermo Fisher Scientific, Waltham, MA, USA) for 30 minutes at 37°C. DRG explants (3–4 DRG explants/cm<sup>2</sup>) and isolated DRG cells (10<sup>4</sup>–10<sup>5</sup>/L) were seeded onto butterfly wings and cultured for 24 hours at 37°C.

### Schwann cell culture

Schwann cells were harvested as previously described (Liu et al., 2019). Briefly, sciatic nerves were isolated from postnatal wild-type rats and green fluorescent protein-transgenic rats and digested with 3 mg/mL collagenase for 30 minutes and 0.125% trypsin for 10 minutes at 37°C. Isolated Schwann cells were cultured in Dulbecco's modified Eagle's medium containing 10% fetal bovine serum (Gibco, Grand Island, NY, USA) and 1% penicillin and streptomycin for 24 hours. Cytosine arabinoside (10 μM; Sigma, St Louis, MO, USA) was added to the cell culture medium for 24 hours, and then 2 μM forskolin (Sigma) and 50 ng/mL heregulin (Sigma) were supplied to the culture media. Cells were then purified by the addition of anti-Thy1.1 antibody (1:1000; Sigma) and rabbit complement protein (1:3; Sigma) to remove contaminating fibroblasts.

### Immunofluorescence staining

DRG explants cultured on the wings of *M.m.* and *P.u.t.* were fixed in 4% paraformaldehyde overnight at 4°C, and incubated in 0.5% Triton X-100 (Sigma) in phosphate-buffered saline, blocked in 5% bovine serum albumin (Thermo Scientific, Rockford, IL, USA) for 1 hour, and incubated in primary antibody, overnight at 4°C. Primary antibody incubations were performed with the following specifications: anti-S100 (a Schwann cell marker; mouse; 1:100; Cat# ab14849; Abcam, Cambridge, MA, USA) and anti-β-tubulin III (a neuron marker; rabbit; 1:100; Cat# ab18207; Abcam). Secondary antibody incubations were performed using goat anti-mouse IgG (Alexa Fluor 594, 1:300; Cat# ab150120; Abcam), donkey anti-rabbit IgG (Alexa Fluor 488, 1:300; Cat# ab150073; Abcam) at 37°C for 2 hours, followed by counterstaining with Hoechst 33342 (1 μg/mL; Sigma). Images were taken by using a scanning confocal microscope (Leica, Wetzlar, Germany).

### Scanning electron microscopy

DRG explants and cells cultured on *M.m.* wings were fixed in 4% paraformaldehyde overnight at 4°C, post-fixed with 1% OsO<sub>4</sub>, gradually dehydrated in acetone, and dried in a critical point drier (Hitachi, Tokyo, Japan). Samples were coated with gold in a JFC-1100 unit (JEOL Inc., Tokyo, Japan) for subsequent observations. Images were taken using a scanning electron microscope (S-3400N; Hitachi).

### Proliferation and adhesion assays

The proliferation rate of Schwann cells was determined using the Cell-Light™ EdU DNA Cell Proliferation Kit (Ribobio, Guangzhou, China). Schwann cells, treated with 50 μM 5-ethynyl-2'-deoxyuridine (EdU) for 24 hours at 37°C, were fixed in 4% paraformaldehyde for 30 minutes and stained with Hoechst 33342 (1 μg/mL; Sigma). Schwann cell adhesion to the wings was detected after 6 hours of culture using 3,3'-diiodoacetylloxycarbocyanine perchlorate (DiO, Invitrogen) fluorescent dye. Images were taken using a Zeiss fluorescence microscope (Axio Imager M2; Jena, Germany).

### In vivo experiments

*M.m.* wings and chitosan film were cut into 1 cm × 1 cm pieces and subcutaneously implanted into the backs of rats, and the blood cellular parameters were assessed using

routine blood tests and histological observations, based on hematoxylin-eosin staining, as previously described (Khalil and Abunasef, 2015; Liu et al., 2016). Peripheral blood samples were collected from the rats 4 weeks after implantation. Various blood cellular parameters, including alanine aminotransferase, aspartate aminotransferase, blood urea nitrogen, creatinine, uric acid, lactate dehydrogenase, alkaline phosphatase, creatine phosphokinase, white blood cells, neutrophil percentages, and lymphocyte percentages, were measured: the values for alanine aminotransferase, aspartate aminotransferase, alkaline phosphatase, and creatine phosphokinase reflected liver function; blood urea nitrogen reflected renal function; creatinine and uric acid reflected kidney function; lactate dehydrogenase indicated cellular status and cell toxicity; and the numbers of white blood cells and the percentages of neutrophils and lymphocytes indicated immune status (Liu et al., 2016; Park et al., 2016). After acid and alkali treatment, *M.m.* wings were immersed in normal saline using various ratios of surface areas to saline volumes to obtain 3, 6, and 12 cm<sup>2</sup>/mL *M.m.* wing extracts. Various concentrations of *M.m.* wing extracts were injected into animals to perform the following tests: intraperitoneal injections into ICR mice were used to perform a systemic acute toxicity test; intradermal injections into the backs of rabbits were used to perform intradermal injection reaction tests; and external applications were used on guinea pigs to perform skin sensitization tests, as previously described (Sun et al., 2019; Sun et al., 2020). A total of 28 specific-pathogen-free ICR mice were randomly divided into four groups (wing male, wing female, normal saline male, and normal saline female groups), containing seven mice in each group. The intraperitoneal cavities of the ICR mice were injected with 6 cm<sup>2</sup>/mL *M.m.* wing extract (50 mL/kg) or normal saline (50 mL/kg). Mice were observed and weighed at 24, 48, and 72 hours after injection. Nine adult white rabbits were randomly divided into three groups (3, 6, and 12 cm<sup>2</sup>/mL *M.m.* wing extracts), containing three rabbits per group. The left back area of each rabbit was intradermally injected with *M.m.* wing extracts at five points (0.2 mL/point) on the left side of the spine, whereas the right back area was injected with normal saline at five points (0.2 mL/point) on the right side of the spine. The reactions observed in the local and surrounding skin, such as erythema, edema, and necrosis, were observed at 24, 48, and 72 hours after injection. *M.m.* wing extracts were externally applied to the left abdomens of guinea pigs to perform the skin sensitization test. In total, 32 adult guinea pigs were randomly divided into four groups (12 cm<sup>2</sup>/mL *M.m.* wing extract, 6 cm<sup>2</sup>/mL *M.m.* wing extract, 4% formaldehyde, and normal saline) containing eight guinea pigs per group. As a positive control, 4% formaldehyde was applied, whereas saline was applied as the negative control. Animal skin reactions at each point were evaluated using the Draize scoring method (Wen et al., 2012). Erythema and edema, the two primary skin parameters that were evaluated, were visually assessed and scored from 0–4. The reaction scores for erythema and edema were added together and divided by two to calculate the primary skin irritation index. The grouping information is shown in **Table 1**.

### Statistical analysis

Data are expressed as the mean ± standard deviation (SD). One-way analysis of variance followed by Dunnett's *post hoc* test for statistical comparisons was performed using GraphPad Prism 5.0 (GraphPad Software, Inc., San Diego, CA, USA).

## Results

### Morphology and growth patterns of DRG neurons

Collected DRG explants containing DRG neurons and the surrounding Schwann cells were immunostained with both the neuron marker  $\beta$ -tubulin and the Schwann cell marker S100. DRG neurons were able to spread and grow on both butterfly

wings, but the cell growth rate and the diffusion directions differed depending on the surface structure morphologies of the butterfly wings. On *M.m.* wing surfaces, which feature grooves, cells grew along the longitudinal structural stripes (**Figure 1**). However, on *P.u.t.* wing surfaces, which feature micro-/nano-concave surfaces, cells grew randomly in all directions (**Figure 1**).

Consistent with immunostaining observations, scanning electron microscopy images also showed that both cultured DRG neurons (**Figure 2A and B**) and DRG explants (**Figure 2C**) displayed good growth behaviors and cellular alignments when cultured on *M.m.* wings.

### Morphology and growth patterns of Schwann cells

Because the dedifferentiation and proliferation of Schwann cells play significant roles in peripheral nerve regeneration (Stierli et al., 2019), the proliferation of Schwann cells on *M.m.* wings was also examined. Schwann cells cultured on *M.m.* wings exhibited EdU-positive signals, indicating that Schwann cells were able to grow and proliferate on *M.m.* wings (**Figure 3**). Schwann cells were also cultured on *P.u.t.* wings and chitosan, which resulted in comparable proliferation rates (**Figure 3**).

In addition to cellular proliferation, the cellular adhesion conditions on *M.m.* wings, *P.u.t.* wings, and chitosan were examined. The attachments of proliferating Schwann cells to two species of butterfly wings and chitosan at different time points (1, 2, and 3 hours) were determined by culturing Schwann cells that express green fluorescent protein. Qualitative observation showed that similar as chitosan, Schwann cells could attach to *M.m.* wings and *P.u.t.* wings (**Figure 4**). DiO labeling also suggested that Schwann cells were able to adhere to *M.m.* wings, *P.u.t.* wings, and chitosan (**Figure 5**).

### Biosafety of *M.m.* wings *in vivo*

The biosafety of butterfly wings in Sprague-Dawley rats was evaluated by examining the effects of the subcutaneous implantation of *M.m.* wings (including untreated and acid and base treated *M.m.* wings) into the backs of rats. Rats showed normal appetites and movement after the subcutaneous implantation of biomaterials. The wounds appeared red and swollen 1 and 2 days after surgery. These symptoms were alleviated with time, and no swelling or suppuration was observed at any time point.

Histological observations showed that, in Sprague-Dawley rats implanted with untreated *M.m.* wings, fibrous connective tissues could be observed wrapping around the implanted *M.m.* wing at 1 week after implantation. At 4 weeks after implantation, the numbers of fibrous connective tissues increased, whereas the numbers of infiltrated inflammatory cells decreased. At 16 weeks after implantation, fewer inflammatory responses were observed, and the untreated *M.m.* wings began to degrade. The degradation of untreated *M.m.* wings was more obvious 24 weeks after implantation (**Figure 6**).

Reduced amounts of fibrous connective tissues wrapping the biomaterial and reduced inflammatory cell infiltration were observed in Sprague-Dawley rats implanted with either treated *M.m.* wings or chitosan compared with rats implanted with untreated *M.m.* wings. In rats implanted with treated *M.m.* wings or chitosan, blood vessel growth and the degradation of biomaterials occurred at earlier time points than in rats implanted with untreated *M.m.* wings, suggesting that treated *M.m.* wings and chitosan induced mild local inflammatory responses and exhibited good compatibility with the surrounding tissues (**Figure 6**).

Peripheral blood samples were collected from Sprague-Dawley

**Table 1 | In vivo assessments of butterfly wing extract buffer**

Group	Intervention	Primary skin irritation index	Response
Systemic acute toxicity test (Institute of Cancer Research mice)			
Wing male (n = 7)	6 cm <sup>2</sup> /mL butterfly wing extract buffer (50 mL/kg)	0	Without toxic symptoms in all four groups
Wing female (n = 7)	6 cm <sup>2</sup> /mL butterfly wing extract buffer (50 mL/kg)	0	
Normal saline male (n = 7)	Normal saline (50 mL/kg)	0	
Normal saline female (n = 7)	Normal saline (50 mL/kg)	0	
Reaction test of intradermal injection (white rabbits)			
12 cm <sup>2</sup> /mL butterfly wing extract buffer (n = 3, left 5 points/rabbit)	12 cm <sup>2</sup> /mL butterfly wing extract buffer (0.2 mL/point)	0	No erythema, edema in all four groups
6 cm <sup>2</sup> /mL butterfly wing extract buffer (n = 3, left 5 points/rabbit)	6 cm <sup>2</sup> /mL butterfly wing extract buffer (0.2 mL/point)	0	
3 cm <sup>2</sup> /mL butterfly wing extract buffer (n = 3, left 5 points/rabbit)	3 cm <sup>2</sup> /mL butterfly wing extract buffer (0.2 mL/point)	0	
Normal saline (n = 9, right 5 points/rabbit)	Normal saline (0.2 mL/point)	0	
Skin sensitization test (guinea pigs)			
12 cm <sup>2</sup> /mL butterfly wing extract buffer (n = 8)	12 cm <sup>2</sup> /mL butterfly wing extract buffer (0.1 mL/point)	0	No erythema, edema
6 cm <sup>2</sup> /mL butterfly wing extract buffer (n = 8)	6 cm <sup>2</sup> /mL butterfly wing extract buffer (0.1 mL/point)	0	No erythema, edema
Positive control (n = 8)	4% formalin (0.1 mL/point)	6	Erythema, edema
Negative control (n = 8)	Normal saline (0.1 mL/point)	0	No erythema, edema

rats 4 weeks after the implantation of treated *M.m.* wings or chitosan, as well as from normal rats. Except for creatine, alkaline phosphatase, neutrophil percentage, and lymphocyte percentage, the other blood parameters of rats injected with treated *M.m.* wings or chitosan were generally consistent with those of normal rats (Table 2). The creatine levels in rats injected with either treated *M.m.* wings or chitosan were much lower than those in rats injected with normal saline, whereas the alkaline phosphatase levels in rats injected with treated *M.m.* wings or chitosan were much higher than those in rats injected with normal saline. These data indicated that implanted biomaterials may induce certain effects on the liver functions of treated animals. The neutrophil percentages increased in rats implanted with treated *M.m.* wings or chitosan, whereas the lymphocyte percentages decreased in rats implanted with treated *M.m.* wings or chitosan, indicating the complexity of biomaterial-induced immune responses.

### Systemic acute toxicity, reactions to intradermal injections, and skin sensitization to *M.m.* wings, in an *in vivo* study

During the 72-hour observation period following intraperitoneal injection, no abnormal phenomena, including vomiting, diarrhea, convulsions, gait instability, or respiratory depression, were observed in any treated ICR mice. No toxic phenomena were observed in any of the ICR mouse groups (Table 1). The body weights of ICR mice slightly increased after 72 hours, and no significant differences were observed between *M.m.* wing extract-treated and normal saline-treated groups or between the two genders (Figure 7).

No skin reactions were detected, and the primary skin irritation index was evaluated for each animal, as previously described (Wen et al., 2012). All rabbits in the 3, 6, and 12 cm<sup>2</sup>/mL *M.m.* wing extract groups received scores of 0 (Table 1).

Any signs of erythema or edema were recorded and scored according to the order of severity. Guinea pigs treated with formaldehyde showed moderate erythema and mild-to-moderate edema (score = 6), whereas *M.m.* wing extract and saline did not trigger any symptoms of skin sensitization when applied to the skin of guinea pigs (score = 0, Table 1).

## Discussion

The surface characteristics of biomaterials can

**Table 2 | Serological effects of butterfly wings and chitosan on Sprague-Dawley rat 4 weeks after implantation**

Parameter	<i>M.m.</i> wings	Chitosan	Normal
Alanine aminotransferase (IU/L)	49.00±2.16	45.66±3.68	42.00±3.26
Aspartate aminotransferase (IU/L)	120.30±6.55	109.33±9.39	137.00±22.70
Blood urea nitrogen (mM)	6.77±0.47	6.99±0.31	6.45±0.73
Creatinine (μM)	20.90±1.18	22.70±2.41	29.30±1.76
Uric acid (μM)	63.67±4.64	55.33±5.73	62.33±3.30
Lactate dehydrogenase (IU/L)	535.30±55.43	520.00±74.31	715.70±131.37
Alkaline phosphatase (IU/L)	307.33±7.76	292.00±10.03	224.33±23.44
Creatine phosphokinase (IU/L)	1374.00±204.71	1323.30±492.9	1297.30±805.9
White blood cells (×10 <sup>9</sup> /L)	0.72±0.10	1.06±0.23	0.51±0.15
Neutrophil percentage	36.00±4.63	39.10±2.60	10.50±1.50
Lymphocyte percentage	52.70±10.61	52.57±7.21	84.27±3.39

Except for creatine, alkaline phosphatase, neutrophil percentage, and lymphocyte percentage ( $P < 0.05$ ), the other blood parameters of rats injected with treated *M.m.* wings or chitosan were generally consistent with those of normal rats. Data are expressed as the mean ± SD and analyzed by one-way analysis of variance with Dunnett's *post hoc* test. Experiments were conducted three times. *M.m.*: *Morpho menelaus*.

influence cellular fates and cellular behaviors, including dedifferentiation, survival, proliferation, attachment, and migration (Stevens and George, 2005; Phillips et al., 2010; Zhou et al., 2013; Kloczko et al., 2015). Butterfly wings, which have delicate surface topological structures, were used as biomaterials to culture Schwann cells and treat peripheral nerve injury (He et al., 2018). In the current study, DRG explants and isolated DRG neurons were also cultured on butterfly wings to observe the effects of butterfly wings on the growth conditions of DRG neurons. Similar to Schwann cells, DRG explants showed diverse growth patterns when cultured on *M.m.* and *P.u.t.* wings, indicating that the surface morphologies of butterfly wings have clear guiding effects on the primary cell types found in the peripheral nervous system. *M.m.* wings, which encouraged the directional growth of Schwann cells and DRG explants, may promote the dedifferentiation and migration of Schwann cells, as well as the elongation of axons, following peripheral nerve

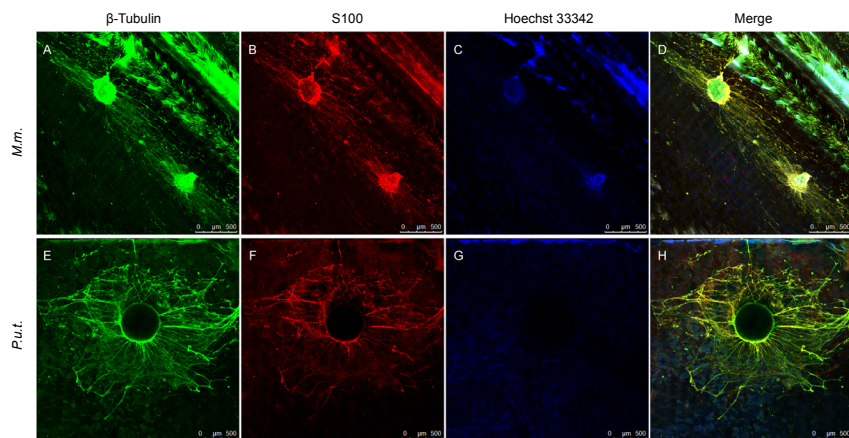


**Figure 1 | Immunostaining of DRG neurons grown on butterfly wings.**

DRG explants were cultured on treated *M.m.* (A–D) and *P.u.t.* wings (E–H) for 24 hours, immunostained with  $\beta$ -tubulin (a neuron marker; green, stained with fluorescein isothiocyanate), S100 (a Schwann cell marker; red, stained with Cy3), and Hoechst 33342 (blue), and subjected to confocal microscopy observations. Scale bars: 500  $\mu$ m. Experiments were conducted three times. DRG: Dorsal root ganglion; *M.m.*: *Morpho menelaus*; *P.u.t.*: *Papilio ulysses telegonus*.

injury, contributing to peripheral nerve regeneration.

The effects of butterfly wings on the cellular phenotypes of Schwann cells, especially cell proliferation and attachment, were also investigated. Schwann cells were cultured on *M.m.* wings, *P.u.t.* wings, and on chitosan, the most widely used biomaterial for neural tissue engineering. The results of the EdU proliferation assay, cell attachment assay, and DiO labeling showed that butterfly wings, particularly *M.m.* wings, resulted in comparable effects as chitosan with regard to cell proliferation and attachment. These results fully demonstrated the biocompatibility of butterfly wings.

Synthetic materials that feature directional lines could also guide the growth of neurons, as shown previously (Bain et al., 2016). Synthetic materials that feature directional lines at various intervals resulted in differing effects on cell growth. The parallel ridges found on *M.m.* wings were spaced approximately 2  $\mu$ m apart, which is a much narrower interval than can be found in most artificial materials. We compared the effects of a chitosan membrane with 30  $\mu$ m parallel ridges with the effects of *M.m.* wings and found that *M.m.* wings appear to be more suitable for the growth of Schwann cells and neurons (unpublished data), indicating the importance of topological structures for cellular behaviors.

In addition to Schwann cell migration and proliferation, the influence of biomaterials on cell dedifferentiation was previously investigated using transcriptome-based network analysis (He et al., 2018). The expression levels of dedifferentiation-associated genes, including Mtor (mechanistic target of rapamycin kinase), Zfp580 (zinc finger protein 580), Jun (Jun proto-oncogene, AP-1 transcription factor subunit), Cacna1g (calcium voltage-gated channel subunit alpha1g), Cdk6 (cyclin-dependent kinase 6), Ncoa3 (nuclear receptor coactivator 3), and Mif (macrophage migration inhibitory

**Figure 2 | Ultrastructure of DRG neurons grown on *M.m.* wings.**

(A) Isolated DRG neurons were cultured on treated *M.m.* wings for 24 hours and subjected to scanning electron microscopy observations. (B) Magnified image of the boxed area in A. The straight line indicates an edge of the *M.m.* wing. The left side shows an *M.m.* wing, whereas the right side shows a plastic petri dish. (C) DRG explants were cultured on treated *M.m.* wings for 24 hours and subjected to scanning electron microscopy observations. DRG explants and isolated cells on *M.m.* wings exhibited a regular sorting pattern, along the parallel ridges. Scale bars: 100  $\mu$ m in A and C; 50  $\mu$ m in B. DRG: Dorsal root ganglion; *M.m.*: *Morpho menelaus*.

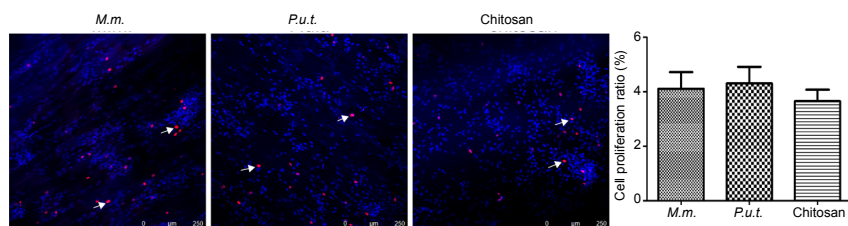
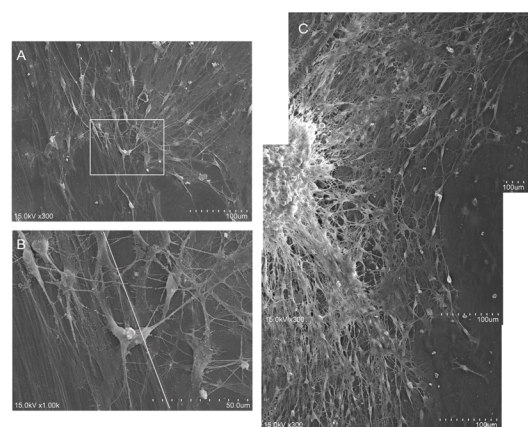


**Figure 3 | The proliferation of Schwann cells on *M.m.* and *P.u.t.* wings.**

The proliferation of Schwann cells cultured on *M.m.* wings, *P.u.t.* wings, and chitosan for 24 hours were determined by the EdU proliferation assay. Cell nuclei are labeled in blue and EdU-positive cells are labeled in red. Arrows indicate new cells. Schwann cells proliferated on both butterfly wing materials and the chitosan membrane, with no significant difference in the proliferation rates of Schwann cells among the three groups ( $P > 0.05$ ). Scale bars: 250  $\mu$ m. Data are expressed as the mean  $\pm$  SD and were analyzed by one-way analysis of variance with Dunnett's *post hoc* test. Experiments were conducted five times. EdU:5-Ethynyl-2'-deoxyuridine; *M.m.*: *Morpho menelaus*; *P.u.t.*: *Papilio ulysses telegonus*.

factor) were examined and compared between cells grown on *M.m.* wings and cells grown on *P.u.t.* wings. Sequencing data showed that the expression levels of these dedifferentiation-associated genes were elevated in cells seeded on *M.m.* wings compared with the levels of these genes in cells seeded on *P.u.t.* wings 0.5, 1, and 3 hours after cell culture (He et al., 2018).

Additionally, *in vivo* studies have previously been conducted to study the biosafety of using butterfly wings as biomaterials as the foundation of constructed tissue-engineered products (Orabi et al., 2013; Sun et al., 2015; Croissant et al., 2018). Several *in vivo* biosafety examinations, including local reaction tests after implantation, acute toxicity tests, intradermal

reaction tests, and skin sensitization tests, have been performed, similar to those described in the present study.

The local reaction experiments use *in vivo* implantation technology to evaluate the biological responses to materials (Sigler et al., 2005; Kuznetsova et al., 2014; Velnar et al., 2016). Histological indicators, including the numbers and distributions of inflammatory cells, fibrosis or the formation of a fibrocystic cavity, and the existence of material debris, are employed to evaluate the toxicity and degradation of implanted materials. Our data showed that the implantation of *M.m.* wings did not induce redness, induration, or necrosis of the skin on the back of Sprague-Dawley rats. Hematoxylin-

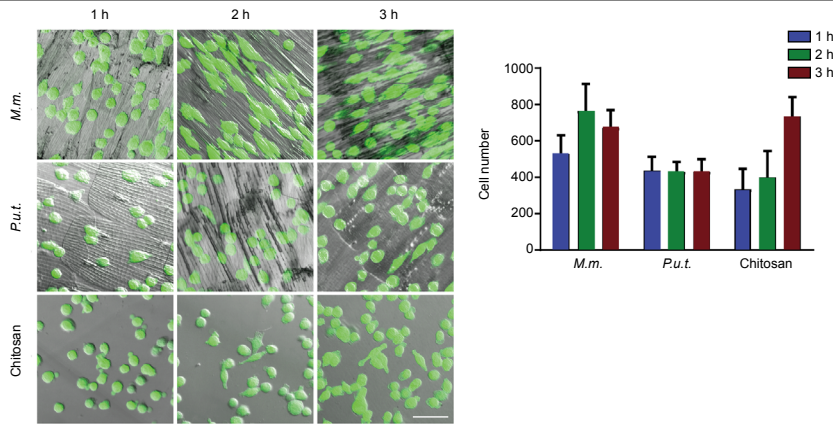


**Figure 4 | The adhesion of Schwann cells on *M.m.* and *P.u.t.* wings.**

The adhesion conditions of Schwann cells cultured on *M.m.* wings, *P.u.t.* wings, and chitosan, 1, 2, and 3 hours after cell seeding. An increased number of Schwann cells attached effectively to butterfly wings during the early culture. Data are expressed as the mean  $\pm$  SD and were analyzed by one-way analysis of variance with Dunnett's *post hoc* test. Scale bars: 50  $\mu$ m. Experiments were conducted five times. *M.m.*: *Morpho menelaus*; *P.u.t.*: *Papilio ulysses telegonus*.

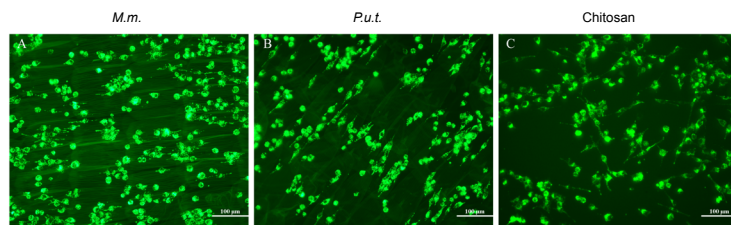


**Figure 5 | The attached Schwann cells on *M.m.* and *P.u.t.* wings after 6-hour culture.**

Schwann cells labeled with DiO were able to survive and grow on both *M.m.* and *P.u.t.* wings, after 6 hours. Scale bars: 100  $\mu$ m. Experiments were conducted three times. DiO: 3,3'-Diocadecyloxycarbocyanine perchlorate; *M.m.*: *Morpho menelaus*; *P.u.t.*: *Papilio ulysses telegonus*.

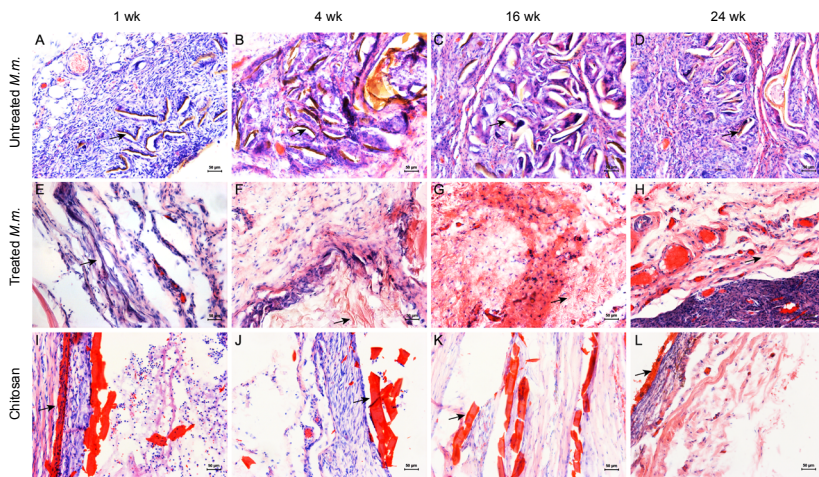


**Figure 6 | Pathological changes after *M.m.* wings were implanted in the backs of Sprague-Dawley rats (hematoxylin-eosin staining).**

Untreated *M.m.* wings (A–D), acid and base treated *M.m.* wings (E–H), and chitosan (I–L) were subcutaneously implanted into Sprague-Dawley rats. Reduced fibrous connective tissue wrapping and inflammatory cell infiltration were observed when treated *M.m.* wings or chitosan was implanted into the rats, compared with untreated *M.m.* wings. At 16 weeks after implantation, the untreated *M.m.* wings began to degrade, which became increasingly apparent 24 weeks after implantation. Moreover, in rats implanted with treated *M.m.* wings or chitosan, the growth of blood vessels and the degradation of biomaterials were observed at earlier time points than with untreated wings. Treated *M.m.* wings or chitosan exhibited mild local inflammatory responses and good compatibility with surrounding tissues. The arrows indicate implanted biomaterials. Scale bars: 50  $\mu$ m. Experiments were conducted three times. *M.m.*: *Morpho menelaus*.

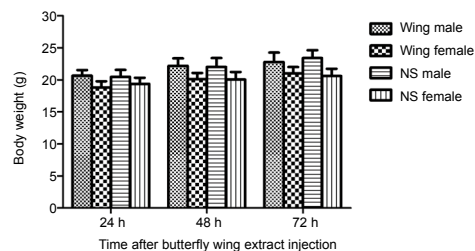


**Figure 7 | Body weights of ICR mice after butterfly wing extract injection.**

The butterfly wing extract or normal saline (NS) control was intraperitoneally injected into ICR mice. The weights of all mice showed a normal upward trend, with no significant difference in weight changes observed for same-sex mice over the same period. Data are expressed as the mean  $\pm$  SD ( $n = 7$ ) and analyzed by one-way analysis of variance with Dunnett's *post hoc* test.

eosin staining results also suggested that *M.m.* wings did not result in rejection or severe inflammatory responses. The observation of blood vessel growth and the degradation of biomaterials indicated that the implanted *M.m.* wings were non-toxic, degradable, and bioactive.

The acute toxicity test is a routine biosafety testing method that examines the influences of biomaterials on organism metabolism and safety (Misik et al., 2015; Hu et al., 2018). ICR mice injected with *M.m.* wing extracts showed no adverse reactions. An increasing trend in body weights was observed among *M.m.* wing extract-injected mice. These outcomes indicated the safety of *M.m.* wings for potential clinical applications.

Additionally, an intradermal reaction test was conducted in rabbits because rabbits tend to have sensitive responses (Gisquet et al., 2011; Diao et al., 2013). A skin sensitization test was conducted using guinea pigs because guinea pigs present a similarly delayed hypersensitivity as that observed in humans (Robinson et al., 1990; Basketter et al., 2008; Basketter et al., 2015). Similar to animals treated with normal saline, no edema, erythema, or other pathological immune responses were detected in animals treated with *M.m.* wing extracts, demonstrating that *M.m.* wing extracts do not contain allergens. However, one weakness of our current study was that we only tested 4% formalin as a positive control in the skin sensitization test but did not use formalin as a positive control for acute toxicity because it may greatly damage the animals. The effects of 4% formalin should also be tested in the systemic acute toxicity test and reaction test of intradermal injection.

Although butterfly wings exhibited good *in vitro* biocompatibility with Schwann cells and DRG neurons and good *in vivo* histocompatibility and biosafety, barriers to the use of butterfly wings in clinical applications still exist. Currently, unlike chitosan, obtaining sufficient amounts of butterfly wings for large scale clinical use may be difficult, which may limit the commercial application of butterfly wings as a biomaterial. However, our current study provided a detailed and reliable experimental basis for future research into bio-mimicking materials for use in neural tissue engineering and regenerative medicine applications.

**Author contributions:** Study design and manuscript writing: JHH, XG; experiment implementation: SW; data analysis: MG; material preparation: YW and CCL. All authors approved the final version of the manuscript. **Conflicts of interest:** The authors declare that they have no conflict of interests.

# Research Article

**Financial support:** This work was supported by the National Natural Science Foundation of China, No.31971276, and the Natural Science Foundation of Jiangsu Higher Education Institutions of China (Major Program), No. 19KJA320005 (both to JHH). The funders had no roles in the study design, conduction of experiment, data collection and analysis, decision to publish, or preparation of the manuscript.

**Institutional review board statement:** The study was approved by the Experimental Animal Ethics Committee of Jiangsu Province, China (approval No.20190303-18) on March 3, 2019.

**Copyright license agreement:** The Copyright License Agreement has been signed by all authors before publication.

**Data sharing statement:** Datasets analyzed during the current study are available from the corresponding author on reasonable request.

**Plagiarism check:** Checked twice by iThenticate.

**Peer review:** Externally peer reviewed.

**Open access statement:** This is an open access journal, and articles are distributed under the terms of the Creative Commons Attribution-NonCommercial-ShareAlike 4.0 License, which allows others to remix, tweak, and build upon the work non-commercially, as long as appropriate credit is given and the new creations are licensed under the identical terms.

## References

- Bain LE, Kirste R, Johnson CA, Ghoshghaei HT, Collazo R, Ivanisevic A (2016) Neurotypic cell attachment and growth on III-nitride lateral polarity structures. *Mater Sci Eng C Mater Biol Appl* 58:1194-1198.
- Basketter D, Darlenski R, Fluhr JW (2008) Skin irritation and sensitization: mechanisms and new approaches for risk assessment. *Skin Pharmacol Physiol* 21:191-202.
- Basketter D, White IR, McFadden JP, Kimber I (2015) Hexyl cinnamal: consideration of skin-sensitizing properties and suitability as a positive control. *Cutan Ocul Toxicol* 34:227-231.
- Bhatt NK, Khan TR, Mejias C, Paniello RC (2017) Nerve transection repair using laser-activated chitosan in a rat model. *Laryngoscope* 127:E253-257.
- Croissant JG, Fatieiev Y, Almalik A, Khashab NM (2018) Mesoporous silica and organosilica nanoparticles: physical chemistry, biosafety, delivery strategies, and biomedical applications. *Adv Healthc Mater* 7:1700831.
- Crosio A, Fornasari BE, Gambarotta G, Geuna S, Raimondo S, Battiston B, Tos P, Ronchi G (2019) Chitosan tubes enriched with fresh skeletal muscle fibers for delayed repair of peripheral nerve defects. *Neural Regen Res* 14:1079-1084.
- Diao JS, Xia WS, Yi CG, Yang Y, Zhang X, Xia W, Shu MG, Wang YM, Gui L, Guo SZ (2013) Histone deacetylase inhibitor reduces hypertrophic scarring in a rabbit ear model. *Plast Reconstr Surg* 132:61e-69e.
- Dietzmeier N, Förthmann M, Grothe C, Haastert-Talini K (2020) Modification of tubular chitosan-based peripheral nerve implants: applications for simple or more complex approaches. *Neural Regen Res* 15:1421-1431.
- Elbaz A, Lu J, Gao B, Zheng F, Mu Z, Zhao Y, Gu Z (2017) Chitin-based anisotropic nanostructures of butterfly wings for regulating cells orientation. *Polymers* 9:386.
- Facklam AL, Volpatti LR, Anderson DG (2020) Biomaterials for personalized cell therapy. *Adv Mater* 32:e1902005.
- Ghosh M, Halperin-Sternfeld M, Adler-Abramovich L (2019) Bio mimicking of extracellular matrix. *Adv Exp Med Biol* 1174:371-399.
- Gisquet H, Liu H, Blondel WC, Leroux A, Latache C, Merlin JL, Chassagne JF, Peiffert D, Guillemin F (2011) Intradermal tacrolimus prevent scar hypertrophy in a rabbit ear model: a clinical, histological and spectroscopical analysis. *Skin Res Technol* 17:160-166.
- Guthrie K, Bruce A, Sangha N, Rivera E, Basu J (2013) Potency evaluation of tissue engineered and regenerative medicine products. *Trends Biotechnol* 31:505-514.
- He J, Sun C, Gu Z, Yang Y, Gu M, Xue C, Xie Z, Ren H, Wang Y, Liu Y, Liu M, Ding F, Leong KW, Gu X (2018) Morphology, migration, and transcriptome analysis of schwann cell culture on butterfly wings with different surface architectures. *ACS Nano* 12:9660-9668.
- Hu LX, Hu SF, Rao M, Yang J, Lei H, Duan Z, Xia W, Zhu C (2018) Studies of acute and subchronic systemic toxicity associated with a copper/low-density polyethylene nanocomposite intrauterine device. *Int J Nanomedicine* 13:4913-4926.
- Khalil WA, Abunasef SK (2015) Can mineral trioxide aggregate and nanoparticulate endosseous root repair material produce injurious effects to rat subcutaneous tissues? *J Endod* 41:1151-1156.
- Kloczko E, Nikkiah D, Yildirim L (2015) Scaffolds for hand tissue engineering: the importance of surface topography. *J Hand Surg Eur Vol* 40:973-985.
- Kuznetsova IV, Maiborodin IV, Shevela AI, Barannik MI, Manaev AA, Brombin AI, Maiborodina VI (2014) Local tissue reaction to implantation of biodegradable suture materials. *Bull Exp Biol Med* 157:390-394.
- Liu C, Kang Y, Zhang H, Zhu L, Yu H, Han C (2016) Establishment of simple and routine methods in early diagnosis of gentamicin-induced kidney injury based on a rat model. *Biomed Res Int* 2016:7160903.
- Liu S, Niu C, Xu Z, Wang Y, Liang Y, Zhao Y, Zhao Y, Yang Y (2019) Modulation of myelin formation by combined high affinity with extracellular matrix structure of electrospun silk fibroin nanoscaffolds. *J Biomater Sci Polym Ed* 30:1068-1082.
- Misik J, Pavlikova R, Cabal J, Kuca K (2015) Acute toxicity of some nerve agents and pesticides in rats. *Drug Chem Toxicol* 38:32-36.
- Mu Z, Zhao X, Xie Z, Zhao Y, Zhong Q, Bo L, Gu Z (2013) In situ synthesis of gold nanoparticles (AuNPs) in butterfly wings for surface enhanced Raman spectroscopy (SERS). *J Mater Chem B* 1:1607-1613.
- Orabi H, Bouhout S, Morissette A, Rousseau A, Chabaud S, Bolduc S (2013) Tissue engineering of urinary bladder and urethra: advances from bench to patients. *ScientificWorldJournal* 2013:154564.
- Park EJ, Lee GH, Yoon C, Jeong U, Kim Y, Cho MH, Kim DW (2016) Biodistribution and toxicity of spherical aluminum oxide nanoparticles. *J Appl Toxicol* 36:424-433.
- Phillips JE, Petrie TA, Creighton FP, Garcia AJ (2010) Human mesenchymal stem cell differentiation on self-assembled monolayers presenting different surface chemistries. *Acta Biomater* 6:12-20.
- Qian Y, Zhou X, Zhang F, Diekwisch TGH, Luan X, Yang J (2019) Triple PLGA/PCL scaffold modification including silver impregnation, collagen coating, and electrospinning significantly improve biocompatibility, antimicrobial, and osteogenic properties for orofacial tissue regeneration. *ACS Appl Mater Interfaces* 11:37381-37396.
- Robinson MK, Nusair TL, Fletcher ER, Ritz HL (1990) A review of the Buehler guinea pig skin sensitization test and its use in a risk assessment process for human skin sensitization. *Toxicology* 61:91-107.
- Sigler M, Paul T, Grabitz RG (2005) Biocompatibility screening in cardiovascular implants. *Z Kardiol* 94:383-391.
- Stenberg L, Kodama A, Lindwall-Blom C, Dahlin LB (2016) Nerve regeneration in chitosan conduits and in autologous nerve grafts in healthy and in type 2 diabetic Goto-Kakizaki rats. *Eur J Neurosci* 43:463-473.
- Stevens MM, George JH (2005) Exploring and engineering the cell surface interface. *Science* 310:1135-1138.
- Sterli S, Imperatore V, Lloyd AC (2019) Schwann cell plasticity-roles in tissue homeostasis, regeneration, and disease. *Glia* 67:2203-2215.
- Sun LC, Su Y, Ding XC, Xu DS, Li CM, Wang L, Li WL, Sun XD, Yu JM, Meng X (2020) In vitro and in vivo evaluation of the safety and efficacy of a novel liquid fiducial marker for image-guided radiotherapy. *Oncol Lett* 20:569-580.
- Sun X, Dai H, Guo P, Sha X (2019) Biocompatibility of a new kind of polyvinyl alcohol embolic microspheres: in vitro and in vivo evaluation. *Mol Biotechnol* 61:610-621.
- Sun Y, Feng W, Yang P, Huang C, Li F (2015) The biosafety of lanthanide upconversion nanomaterials. *Chem Soc Rev* 44:1509-1525.
- Velnar T, Bunc G, Klobucar R, Gradisnik L (2016) Biomaterials and host versus graft response: a short review. *Bosn J Basic Med Sci* 16:82-90.
- Vermeulen S, de Boer J (2020) Screening as a strategy to drive regenerative medicine research. *Methods* doi:10.1016/j.jmeth.2020.04.004.
- Wang X, Hu W, Cao Y, Yao J, Wu J, Gu X (2005) Dog sciatic nerve regeneration across a 30-mm defect bridged by a chitosan/PGA artificial nerve graft. *Brain* 128:1897-1910.
- Wen MM, El-Kamel AH, Khalil SA (2012) Systemic enhancement of papaverine transdermal gel for erectile dysfunction. *Drug Dev Ind Pharm* 38:912-922.
- Yi S, Xu L, Gu X (2019) Scaffolds for peripheral nerve repair and reconstruction. *Exp Neurol* 319:112761.
- Yu HD, Zhang L, Xia LY, Mao M, Ni XB, Leng WD, Luo J (2020) Construction and characterization of nano-hydroxyapatite/chitosan/polycaprolactone composite scaffolds by 3D printing. *Zhongguo Zuzhi Gongcheng Yanjiu* 24:1496-1501.
- Yu JZ, Korkmaz E, Berg MI, LeDuc PR, Ozdoganlar OB (2017) Biomimetic scaffolds with three-dimensional undulated microtopographies. *Biomaterials* 128:109-120.
- Zhang F, Shen Q, Shi X, Li S, Wang W, Luo Z, He G, Zhang P, Tao P, Song C, Zhang W, Zhang D, Deng T, Shang W (2015) Infrared detection based on localized modification of Morpho butterfly wings. *Adv Mater* 27:1077-1082.
- Zhou J, Sui F, Yao M, Wang Y, Liu Y, Tian F, Li Q, He X, Shao L, Liu Z (2013) Novel nanometer scaffolds regulate the biological behaviors of neural stem cells. *Neural Regen Res* 8:1455-1464.

C-Editor: Zhao M; S-Editors: Yu J, Li CH; L-Editors: Giles L, Yu J, Song CP; T-Editor: Jia Y